IONIC CONDUCTIVITY STUDIES OF YTTRIA DOPED CERIA SOLID SOLUTIONS

R.A. Montalvo[1*], S.M. Costilla[1], Sagrario M. Montemayor[1], K.P. Padmasree[2], A.F.Fuentes[2]

[1]Facultad de Ciencias Químicas, Universidad Autónoma de Coahuila, Blvd. V. Carranza esq. J. Cárdenas, Saltillo, Coahuila, México. C.P. 25280.
[2]Cinvestav-Saltillo, Carretera Saltillo-Monterrey Km.13, Ramos Arizpe, Coahuila, México. C.P. 25900

*Tel (844) 4389612, Fax (844) 4389610, broodover@hotmail.com

ABSTRACT

In this paper we report the electrical conductivity studies for yttria doped ceria $Ce_{1-x}Y_xO_{2-\delta}$, (where $0 \leq x \leq 0.2$), prepared at room temperature by mechanically milling from the stoichiometric mixtures of the corresponding oxides. Electrical conductivity measurements were performed by using pressed pellets sintered at 1500°C as a function of frequency and temperature. It was found that the electrical conductivity of the sample increases with the addition of yttria dopant and maximum bulk conductivity (2.72×10^{-2} S/cm) obtained for $Ce_{0.8}Y_{0.2}O_{1.9}$. The frequency dependence of the σ_{ac} of these oxide ion conductors showed a remarkably different behavior from that of the cation ones. The ac conductivity σ_{ac} in the low frequency range was strongly influenced by space charge polarization at grain boundary and the high frequency plateau agreed with the bulk conductivity of the system. Two dielectric relaxations observed the in the dielectric loss spectra corresponds to the ionic conductive process of bulk and grain boundaries.

Tópico: Celdas de Combustible

Modalidad: Oral

1.-Introduction

The solid oxide fuel cells (SOFCs) have many advantages such as high efficiency and material compatibility among the various types of fuel cells [1,2]. The solid oxide electrolyte is the key component which plays the role of the oxygen ion conductor at high temperature. In oxygen ion conducting solid electrolytes, current flow occurs by the movement of oxygen ions through the crystal lattice as a result of thermally activated hopping of the oxygen ions moving from a crystal lattice site to another crystal lattice site. Currently yttria stabilized zirconia (YSZ) is widely used as an electrolyte due to its outstanding chemical and mechanical stabilities but it requires high operating temperatures (1000°C) to achieve sufficiently high conductivity. High operating temperature of YSZ electrolyte can lead to complex material problems such as electrode sintering, interfacial diffusion between electrolyte and electrodes, and mechanical stress due to different thermal expansion coefficients. Therefore, development of solid electrolytes that can be used in intermediate temperature (e.g., 600-800°C) is important for the future growth of SOFC technology [3-5]. One of the methods to reduce the operating temperature is to use new electrolyte materials which have higher oxygen ionic conductivity. Cerium based solid solutions have been recognized to be the most promising electrolytes for intermediate temperature SOFC (IT-SOFC), since their ionic conductivity is higher than YSZ at the intermediate temperature range. Ceria oxide (CeO_2) is a fluorite structured ceramic material which does not show any known crystallographic change from room temperature up to its melting point. The oxygen vacancies are created in the CeO_2 lattice for charge compensation when doped with rare earth and alkaline earth materials.

The frequency dependent properties of a material can be described via four interrelated complex plane methods, complex impedance (Z^*), complex admittance $(Y^*=1/Z^*)$, complex permittivity $(\varepsilon^*=1/(j\omega C_0 Z^*))$ and complex modulus $(M^*=j\omega C_0 Z^*)$. Here j=$\sqrt{-1}$, ω (= $2\pi f$) is the angular frequency and $C_0=\varepsilon_0 A/d$, is the geometrical capacitance of the cell with the dielectric medium being replaced by free space (vacuum), $\varepsilon_0=8.854\times10^{-14}$ F/cm is the permittivity of free space, and d and A are the thickness and area of the sample. Analysis of such data provides an insight into the detailed microscopic process in the full electrode and bulk material system. For solid oxide fuel cell applications, it may be useful to investigate

the conduction mechanism of oxide ions in the electrolyte system. Many studies have been performed on ac conductivity measurements in order to explain ion dynamics of oxide ion conductors. It is well known that the ac conductivity (σ_ω) of many cation conductors obeys the following relation

$$\sigma_{(\omega)} = \sigma_0 + A\omega^n \qquad (1)$$

where σ_0 represents σ_ω extrapolated to zero frequency, which corresponds to the dc conductivity (σ_0), ω is the angular frequency, and A is a constant. The power law exponent n $(0 \leq n \leq 1)$ is determined by the strength of the ion-ion interactions in the ionic hopping process; i.e. in the absence of interactions among mobile ions (completely independent and random ion hopping), the exponent n would be zero. This relation is known as Universal Dielectric Response (UDR) and is applied to many cation conductors having either crystal or glass structures [6]. On the other hand, only a few studies concerning the conductivity dispersion of oxide ion conductors have been reported. In the present work, yttria doped ceria $Ce_{1-x}Y_xO_{2-\delta}$, (where $0 \leq x \leq 0.2$) system is prepared at room temperature by mechanically milling technique. The electrical properties have been studied in order to understand the ionic transport mechanism in $Ce_{1-x}Y_xO_{2-\delta}$ (where $0 \leq x \leq 0.2$) system in the temperature range 200-800°C.

2.- Experimental conditions

Powder samples of $Ce_{(1-x)}Y_xO_{2-\delta}$, (where $0 \leq x \leq 0.2$) were synthesized by mechanical milling, using high purity (Aldrich, >99+%) CeO_2 and Y_2O_3 as starting materials. Stoichiometric mixtures of the above chemicals were placed in zirconia containers together with 20 mm diameter zirconia balls as grinding media (balls to powder mass ratio = 10:1). Dry mechanical milling was carried out in air in a planetary ball mill by using a rotating disc speed of 350 rpm. Phase evolution on milling was analyzed by using X-ray powder diffraction in Philips X'pert Diffractometer using Ni-filtered CuK_α radiation (λ=1.5418Å) in the range of 2θ =20-80°. The morphological features of the particle were observed using a scanning electron microscope (SEM) Philips XL 30ESEM. The experimental method most frequently used for measuring the electrical characteristics is the complex impedance

method, and is used almost exclusively in the area of ionic conduction in solids. Specimens for electrical property measurements were pellets obtained by pressing the sample powder in a hydraulic press at a pressure of 5MPa and sintered at 1500^{o}C for 2 hr, with a diameter of 10 mm diameter and ~ 1 mm thickness. The two electrodes were formed by applying platinum paste to either surface of the pellets and then heat treated at 600°C for two hours before the measurement to burn out the binder of the platinum paste and to ensure good contact of the electrodes with the pellet. The transport properties of the sintered pellets were examined by ac impedance spectroscopy over a frequency range 100Hz to 1MHz using Solartron 1260 Frequency Response Analyzer. Temperature and frequency dependence of electrical properties were studied in the frequency range 100 Hz to 1MHz and temperature range 200-800°C.

3.- Results and discussion

The XRD patterns were measured for all the doped ceria samples after 1 hr of dry milling at room temperature to ensure the complete dissolution of Y_2O_3 into CeO_2. Fig.1. shows the powder X-ray diffraction pattern after 1 hr milling of $Ce_{(1-x)}Y_xO_{2-\delta}$ confirms the formation

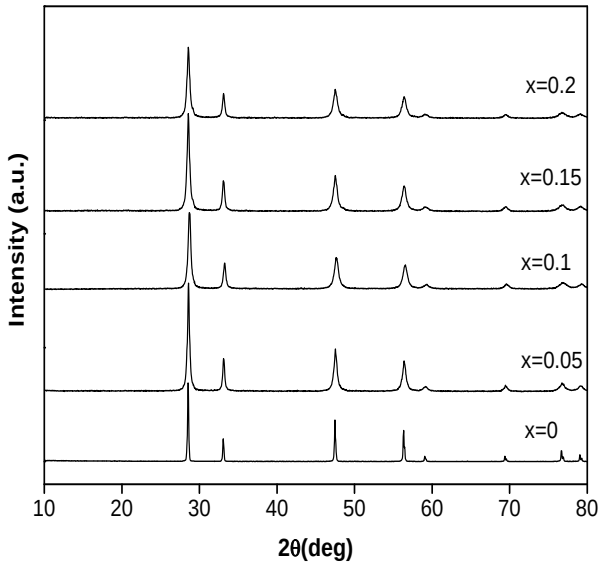

Fig.1. XRD patterns $Ce_{(1-x)}Y_xO_{2-\delta}$ solid solutions after 1 hr milling.

of single phase cubic fluorite structure. Any additional phase corresponding to yttria is not observed, suggesting that the compound is having a single phase cubic structure. The dissolution of Y_2O_3 in the cubic fluorite structure causes a slight shift in ceria peak. This shift is indicative of change in lattice parameter. The lattice constant of $Ce_{(1-x)}Y_xO_{2-\delta}$ increased linearly with the dopant content and is shown in Table 1. This is because the ionic radius of Y^{3+} (0.1019 nm) are slightly greater than that of Ce^{4+} (0.097 nm), so the substitution of Ce^{4+} with Y^{3+} in the lattice of CeO_2 would increase the magnitude of crystal lattice.

Electrical properties of the doped system generally depend on the microstructural features. Fig.2 (a) and (b) shows the SEM micrographs of $C_{e0.8}Y_{0.2}O_{1.9}$ milled sample and sample sintered at 1500°C for 2 hr. Fig. 2(a) shows the sample prepared by mechanical milling had a uniform particle size distribution and well crystalline shape. Sintering at 1500°C resulted in sub-micrometer grain size. The sintered specimen presents uniform grain size, highly dense microstructure with little pores. Similar images are also found in other yttria doped ceria samples.

(a) (b

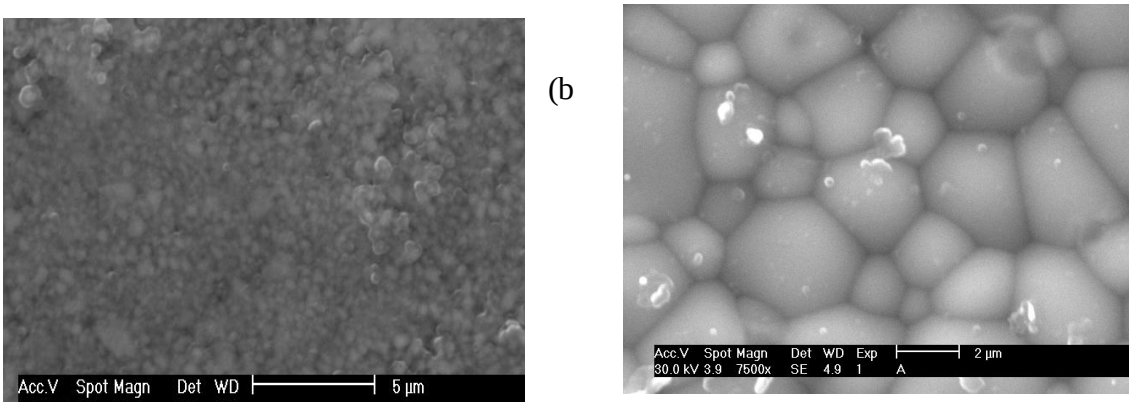

Fig.2. Scanning electron micrograph of $Ce_{0.8}Y_{0.2}O_{1.95}$ (a) prepared by ball milling and (b) sample sintered at 1500°C for 2 hrs

The impedance measurement is a well-developed tool to separate out the bulk and grain boundary contribution to the total conductivity. The impedance spectrum is usually

represented as the negative of imaginary component of impedance $(-Z'')$ versus real component of impedance (Z'), which is referred as the Nyquist plot. Typically, the plot would be composed of three semicircles, each semicircle representing a distinct process whose time constant is sufficiently separated from the others over the range of measurement frequencies. The semicircles at higher, intermediate and lower frequencies represent bulk, grain boundary and electrode process. The complex impedance plot for $Ce_{0.8}Y_{0.2}O_{1.95}$ material at different temperatures is shown in figure 3. With the increase in temperature both the bulk and grain boundary resistance decreases indicating an increase in both the bulk and grain boundary conductivities which results in increase of the total ionic conductivity of the material. From the figure we can see at low temperatures an incomplete arc at low frequencies and another one at high frequencies associated with the bulk contribution. The real axis intercept of the high and low frequency arc gives the value of bulk and grain boundary resistance associated with the sample. The bulk dc conductivity was easily obtained from the conductivity value at high frequency plateau of the ac conductivity plot. At elevated temperature, the bulk effects move out the experimental frequency window, and grain boundary and electrode-electrolyte interface effect come into

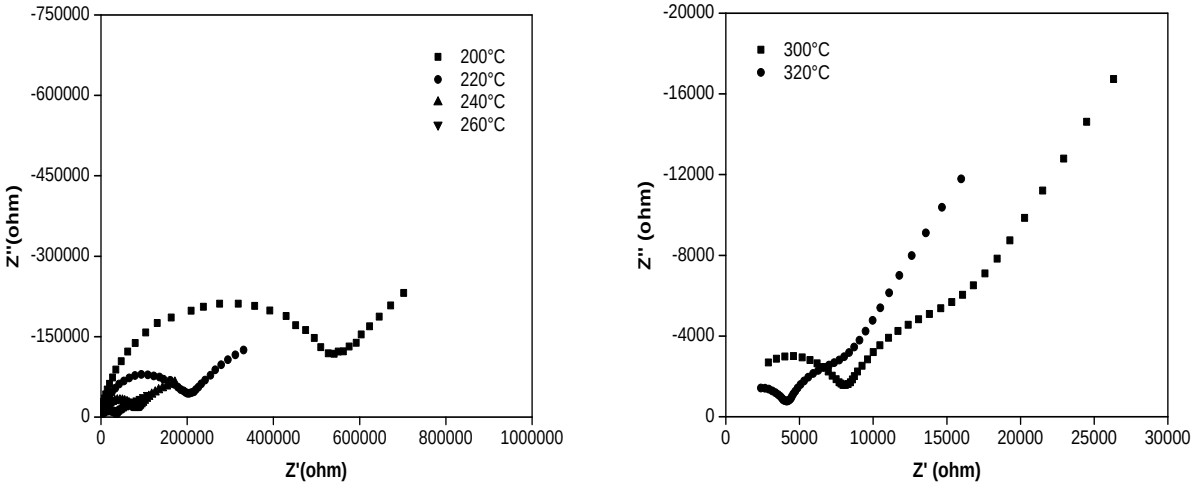

Fig.3. Impedance spectra of yttria doped ceria solution at different temperatures

the frequency spectrum. The presentation of the impedance spectra generally allows a clear separation of the different processes in ionic conducting sample. The temperature dependence of the bulk conductivity for $Ce_{1-x}Y_xO_{2-\delta}$ as well as for 8YSZ measured in air are shown in the figure 4. The temperature dependence of conductivity can be described by Arrhenius law of the form, $\sigma = \sigma_0 \exp\left(-\frac{E_a}{kT}\right)$,where σ_0 is the pre-exponential factor which is related to the effective number of mobile oxygen ions and E_a is the activation energy for oxide ion conduction. The ionic conductivity increases with the increase in temperature, where as the difference in ionic conductivity decreases as the temperature increases. This result confirms that the mobility of the oxide ion makes a dominant contribution to the ionic conduction [8].

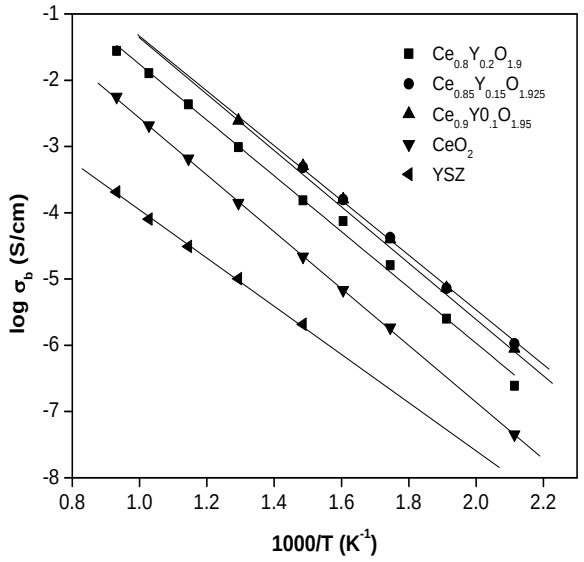

Fig.4. Temperature dependence of the bulk conductivity of $Ce_{1-x}Y_xO_2$ and YSZ samples

The activation energies for oxygen ion migration in $Ce_{(1-x)}Y_xO_{2-\delta}$ system at different temperatures were calculated from the slope of the Arrhenius plot (logσ versus1/T) and is given in the table.1. Fig.5. shows the bulk conductivity against Yttrium contents at three different temperatures. The bulk ionic conductivity of $Ce_{(1-x)}Y_xO_{2-\delta}$ increases as the Yttrium substitution increases and the ionic conductivity reaches a maximum value (2.72×10^{-2}

S/cm) for $Ce_{0.8}Y_{0.2}O_{1.9}$ at 800°C. In the high temperature range of 600-800°C, x=0.2 have the higher ionic conductivity than those of the other yttria doped system.

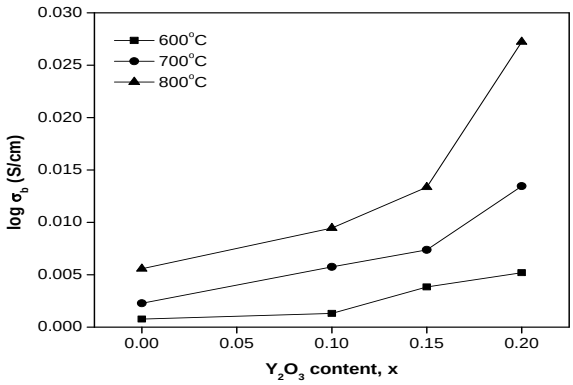

Fig.5. Bulk conductivity versus Y^{3+} content at three different temperatures.

Table 1. The lattice constant, bulk conductivity (σ_b) (S/cm) and activation energy (eV) obtained at 600°C, 700°C and 800°C for $Ce_{(1-x)}Y_xO_{2-\delta}$

CeO_2	0.54124	7.66×10^{-4}	2.28×10^{-3}	5.58×10^{-3}	0.851
$Ce_{0.9}Y_{0.1}O_{1.9}$	0.54240	1.32×10^{-3}	5.76×10^{-3}	9.45×10^{-3}	0.849
$Ce_{0.85}Y_{0.15}O_{1.925}$	0.54303	3.84×10^{-3}	7.38×10^{-3}	1.33×10^{-2}	0.845
$Ce_{0.8}Y_{0.2}O_{1.9}$	0.54366	5.20×10^{-3}	1.35×10^{-2}	2.72×10^{-2}	0.833

Fig.6. shows the ac conductivity as a function of *log f* at various temperatures for the sample $Ce_{0.15}Y_{0.85}O_{1.925}$. Similar conductivity plots were obtained for all samples analyzed in this work. The conductivity plots strongly depend on the measuring temperatures. From the figure we can see in the temperature range below 300°C, there is only one plateau region associated with the dc conductivity σ_{dc} and a high frequency dispersion following the power law exponent [7]. This behavior has been linked with the existence of cooperative effects in the dynamics of hopping ions. The frequency dispersions both at low and high frequencies shift to higher frequencies with increase of temperature. The temperature range from 300°C to 400°C shows the presence of two plateaus, which are frequency independent in the low and high frequency region. The appearance of low frequency plateau is due to the blocking effect of grain boundaries which show prominent

effect at low frequencies. But the spectra obtained at 500°C and above showed only one plateau as the high frequency plateau region shifts to still higher frequencies and it are beyond the measurement range of present study.

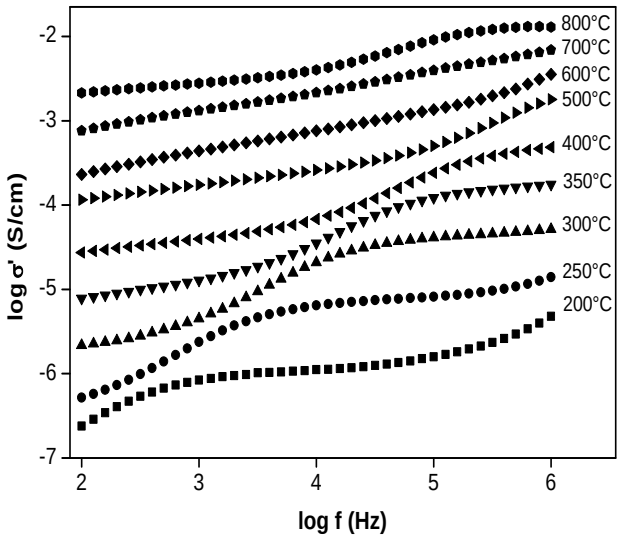

Fig.6. Real part of the conductivity versus frequency at various temperatures for $Ce_{0.15}Y_{0.85}O_{1.925}$.

In the high temperature range, the conductivity value estimated from the low frequency plateau did not agree with that of bulk conductivity, but agreed with the total conductivity estimated from the bulk and grain boundary from the impedance spectra. The conductivity value estimated from the high frequency plateau agreed with the bulk conductivity obtained form the impedance spectra. The conductivity dispersion in the intermediate frequency range is high for the material having higher grain boundary resistivity than the bulk resistivity as shown in Fig.6. So we can assume that the plateau in the low frequency range for the temperature above 300°C is due to the polarization of space charge due to the presence of larger grain-boundary barrier. This means that one part of the mobile oxide-ions contributes to oxide ion conduction and the other part does to the polarization at the grain boundary barrier as the space charge. But in the high frequency range, the charge can follow no longer with the frequency; the plateau at the high frequency corresponds to bulk conductivity.

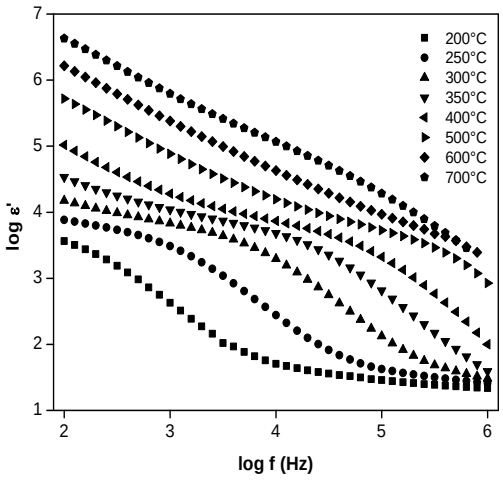

Fig.7. Dielectric constant ε′ versus frequency for $Ce_{0.85}Y_{0.15}O_{1.925}$ at different temperatures.

Fig.7. shows frequency dependence of dielectric constant ε′ at various temperatures. At low temperatures, i.e. at and below 400°C, the data exhibit frequency dispersion and a low frequency shoulder corresponding to the limiting low frequency dielectric constant, ε_0. After 400°C, the ε′ values rapidly increases at lower frequencies. This is due to a space charge polarization effect, because of the ionic conductor/metallic electrode blocking interface, and to the increase in the dc conductivity of the material. This behavior is quite common for the dielectric spectra of complex ionic conductors. The dielectric dispersion observed at intermediate frequencies may be due to the grain boundary effect. Such dispersion at intermediate frequencies was also observed in Y doped ZrO_2, which may be attributed to grain boundary effects [9]. Fig.8 shows the relationship between the dielectric loss angle and the applied frequency at different temperatures. The figure shows the presence of two distinct dielectric relaxation peaks. Only one high frequency relaxation peak is observed for the temperatures 200, 250 and 300^{o}C but the spectra at 350 and 400^{o}C clearly shows the presence of two relaxation peaks but it is beyond the measuring limit of the present study. It was found that the relaxation peaks shift to higher frequency region and the peak height increases with increase in temperature. The fact that this spectrum contains two relaxation peaks is important evidence for relaxations due to the ionic transport process of the bulk and grain boundary region. The two conduction components in

the impedance spectra confirm the exhibition of two dielectric relaxation peaks due to bulk and grain boundary.

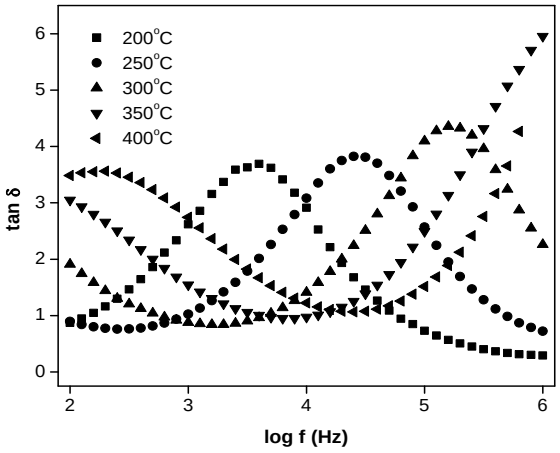

Fig.8. Tan δ versus frequency for $Ce_{0.85}Y_{0.15}O_{1.925}$ at different temperatures.

The relaxation time τ in dielectric studies is given by the resonant condition $2\pi f\tau=1$, where f is the resonant frequency obtained from the dielectric relaxation spectra. The relaxation time obtained at 200°C, 250°C and 300°C are 3.99×10^{-5}, 6.33×10^{-6} and 1.00×10^{-6}. The dielectric result provides a direct evidence of grain boundary effects in oxygen ionic conductors.

4.-Conclusions

The solid solutions of CeO_2-Y_2O_3 have been successfully prepared at room temperature via mechanochemical synthesis. The X-ray diffraction pattern confirms the cubic fluorite structure after 1 hr of milling. The addition of yttrium oxide to ceria results in structural changes in the crystal lattice and changes in the ionic conductivity. Electrical conductivity measurements showed that the conductivity increases with the increase in dopant amount and a maximum conductivity is obtained for 0.2mole% of yttria doped ceria. The ionic conductive process of the bulk and grain boundary is well documented in the dielectric relaxation spectra. Doped ceria appears to be a promising solid electrolyte alternative to

doped zirconia because of its high conductivity for application at intermediate temperatures.

5.-Acknowledgements

The authors thanks to Conacyt for the financial support.

6.-References

[1] H. L. Tuller, A. S. Nowick, *J. Electrochem. Soc.* 122, 255, (1975).

[2] H. Yahiro, Y.Baba, K. Eguchi, H. Arai, *J. Electrochem. Soc.* 135, 2088, (1988).

[3] Chun Tian, Siu-Wai Chan, *Solid State Ionics* 134, 89, (2000).

[4] Jan Van Herle, T Horita, T. Kawada, N. Sakai, H. Yokokawa, M. Dokiya, *J. Europ. Ceram. Soc.* 16, 961, (1996).

[5] H. Yamamura, S. Takeda, K. Kakinuma, *J. Ceram. Soc. Jap.* 115, 4, 264 (2007).

[6] A.K. Jonscher, *Nature* 267, 673, (1977).

[7] A.K. Jonscher, *Dielectric relaxation in solids*, Chelsea Dielectric Press, London (1984).

[8] S. Dikmen, P. Shuk, M. Greenblatt, H. Gocmez, *Solid State Sci.* 4, 585, (2002).

[9] A. Pimenov, J. Ullrich, P. Lunkenheimer, A Loidl, C.H. Ruscher, *Solid Sate Ionics* 109, 111, (1998).